

EFFECT OF ANNEALING ON THE ELECTRICAL AND OPTICAL PROPERTIES OF $\text{Cu}_5\text{Ga}_{33}\text{Te}_{62}$ THIN FILM

D. GHONEIM, K. H. MARZOUK^a, S. N. EL-SAYED, N. A. MOHSEN,
A. M. A. MAHMOUD*

Faculty of Science, Physics Department, Al-Azhar University (Girls), Cairo, Egypt

*^aPhysics Department, National Center for Radiation Research and Technology,
Nasr City, Cairo, Egypt*

Thin film of $\text{Cu}_5\text{Ga}_{33}\text{Te}_{62}$ system has been prepared by using thermal evaporation technique with 45 nm thickness. The electrical conductivity assessment has been carried out on this film in the temperature range of 300- 425 K. The film has been annealed at 323, 348, 373, 398, 423 and 453 K under vacuum for 3 hr. The temperature dependence of the electrical conductivity for all annealing temperatures has been recorded and discussed. The results were analyzed in order to establish the activation energy of each state. With the increase in the annealing temperature the film undergoes phase transition to the crystalline state. The optical properties of $\text{Cu}_5\text{Ga}_{33}\text{Te}_{62}$ system have been studied as a function of annealing temperature. The results showed that the optical transitions in the wave length range (200- 1100) nm are direct transitions where the values of E_g are decreased with increasing annealing temperature, i.e., the absorption edge shifts toward a higher wavelength or a lower energy. The optical constants k , n , ϵ_r and ϵ_o of the film at different temperatures are influenced by the heat treatment.

(Received April 10, 2010; accepted April 27, 2010)

Keywords: Cu-Gsa-Te, Thin film, Annealing, Optical properties, Electrical properties

1. Introduction

Amorphous chalcogenide films have potential and current application in optical memories, photonics crystals and optics. Optically or electrically recorded memories are currently 'hot' scientific topics. In recent years, efforts are being made to develop chalcogenide-based rewritable optical memories [1]. The optical properties of amorphous semiconductors have been the subject of many recent papers. It is well known that the optical gap of amorphous semiconductor alloys strongly depends on their compositions. The study of the optical constants of materials has been interesting for many reasons. First, the use of materials in optical fibers and reflected coating requires accurate knowledge of their optical constants over wide ranges of wavelength. Second, the optical properties of all materials are related to their atomic structure, electronic band structure and electrical properties [2]. The structural bonding between the neighbors determines the optical properties, such as absorption and transmission of the amorphous material. The general features of the density of states of amorphous solids can be obtained from the model proposed by Mott and Davis [2,3]. Thermal processes are known to be important in inducing crystallization in semiconducting chalcogenide glasses. Crystallization of chalcogenide films is accompanied by a change in the optical band gap. Separation of different crystalline phases with thermal annealing has been observed in ternary glasses. The effect of thermal annealing is interpreted on the basis of amorphous crystalline transformation [1].

*Corresponding author: mohsen.nadia@yahoo.com

In the present work we determine the activation energy, optical band gap, absorption coefficient (α), refractive index (n) and extinction coefficient (k) for $\text{Cu}_5\text{Ga}_{33}\text{Te}_{62}$ thin film annealed at different temperatures (323,348,373,398,423 and 453 K). The optical properties were determined by using transmission and reflection data spectra in the wavelength range 200–1100 nm.

2. Experimental

The compound was prepared in bulk form by the melt quenching method. A mixture of highly pure components Cu, Ga, and Te (99.999%) in their stoichiometric ratio were weighted and placed in evacuated silica tube under vacuum 10^{-6} Torr (at the national research center). The ampoule was heated in a rotating furnace and raised gradually up to 1200 C^0 and then kept at this temperature for 24 hrs to ensure a high degree of homogeneity. The melt was quenched in ice water to obtain the film in the bulk form. $\text{Cu}_5\text{Ga}_{33}\text{Te}_{62}$ thin film with thickness 45 nm has been obtained by thermal evaporation onto ultrasonically glass substrate by using Edward E 306 coating unit under vacuum 10^{-6} Torr with low deposition rate (at the National Center for Radiation Research and Technology). The thickness has been controlled by crystal oscillator monitor (Moaxtek TM-200). The composition of the film was analyzed by EDAX which showed that the ratios of the elements of the film are in good agreement with the bulk as shown in Fig. 1. X-ray diffraction investigations were carried out to identify the structure of the obtained materials in bulk and thin film form before and after annealing at 453 K. The annealing was carried out under vacuum 10^{-3} Torr for 3 hrs at different temperatures (323,348,373,398,423 and 453 K). The structural properties of the evaporated $\text{Cu}_5\text{Ga}_{33}\text{Te}_{62}$ thin film were investigated by X-ray diffraction (using Xpert ProPan analytical diffractometer instrument with copper CuK_α radiation ($\lambda=1.54\text{ \AA}$)). The X-ray diffraction pattern was obtained in the range $10^\circ\text{--}90^\circ$ (2θ , $0.02^\circ/\text{step}$ increments). The electrical conductivity was recorded for thin films as a function of temperature in the range 300–425 K. This step was repeated after each annealing temperature. The normal incidence and absorption spectra of the thin film at different temperatures were measured in the range 200–1100 nm by using a double beam spectrophotometer (Shimadzu model UV-160A). All optical measurements were performed at room temperature. The obtained absorption data against incident light wavelength were used to calculate the optical energy gap and optical constant.

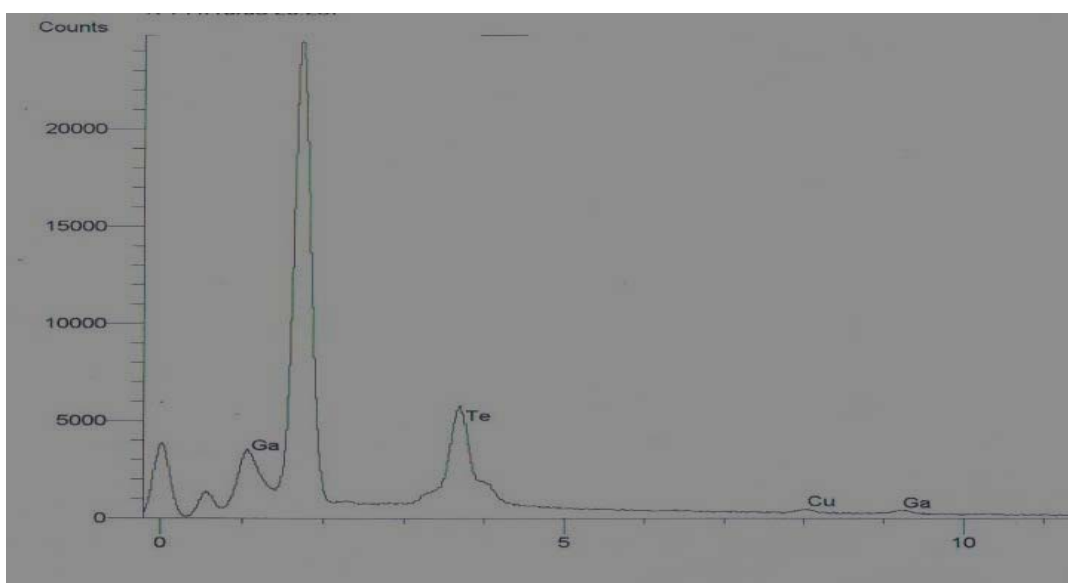


Fig.1. EDAX analysis of the composition of $\text{Cu}_5\text{Ga}_{33}\text{Te}_{62}$ thin film

3. Results and discussion

3.1 structure properties

The optical properties of $\text{Cu}_5\text{Ga}_{33}\text{Te}_{62}$ film being annealed for different temperatures T_a were studied in this work. The XRD analysis showed that the structure of the film changed from the amorphous state in the as-deposited film to a partial crystalline phase in the annealed film at 453 K as indicated in Fig. 2. The values of the d-spacing of the annealed film at 453 K are compared with the international data calculated from ICSD using POWD-12++ [1997] card number 79-20331. Table 1 shows this comparison which indicates matching with $\text{Cu}_5\text{Ga}_{33}\text{Te}_{62}$ phase.

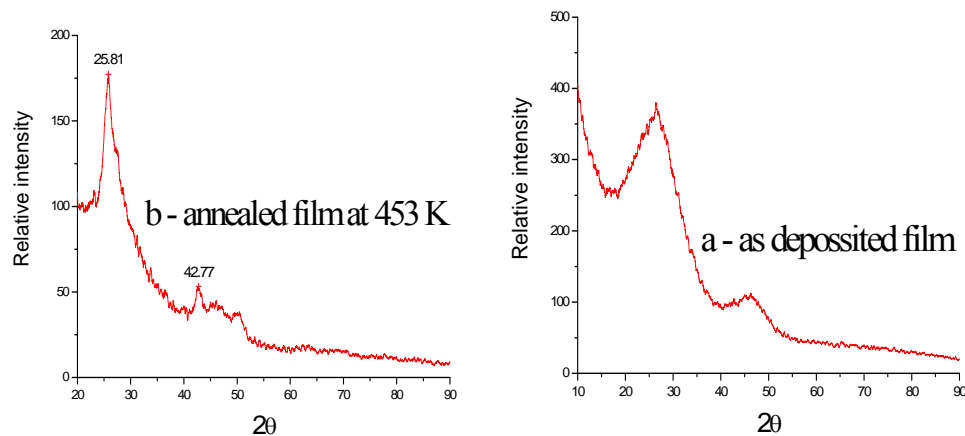


Fig.2 a,b the XRD pattern of as-deposited and annealed $\text{Cu}_5\text{Ga}_{33}\text{Te}_{62}$ thin film at 453 K, respectively.

Table 1. the d-spacing of the $\text{Cu}_5\text{Ga}_{33}\text{Te}_{62}$ annealed thin film at 453 K.

No	Intensity	d-spacing	ICSD data	Matching	Phase
1	100	3.463	3.467	79-2331	CuGaTe_2
2	25	2.1167	2.12	79-2331	CuGaTe_2
3	19	1.810	1.8146	79-2331	CuGaTe_2

3.2 Electrical conductivity

The D.C conductivity was recorded as a function of temperature in the range 300-425 K. The D.C conductivity dependence on temperature was measured after each annealing temperature according to the Arrhenius equation [1]

$$\sigma = \sigma_0 \exp\left(\frac{-\Delta E_\sigma}{K_B T}\right) \quad (1)$$

where σ_0 is the pre-exponential factor, ΔE_σ is the activation energy and K_B is the Boltzmann constant. The thermal activation energy of the films was determined from the slopes of $\ln \sigma$ versus $1/T$ plots of equation 1 as shown in Fig. 3. It can be seen that the conductivity increases with the annealing temperature and shows two slightly straight lines indicating two temperature regions, the low temperature region from 300-352 K, and high temperature region from 352-453 K. The calculated activation energies of each regions as a function of annealing temperature are shown in

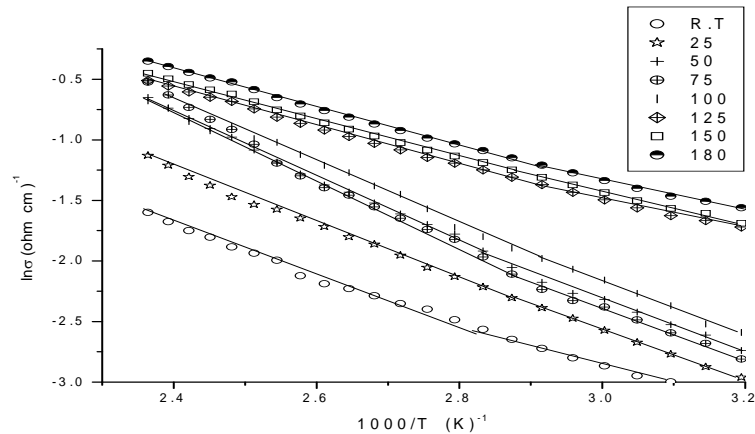


Fig. 3. The relation between $\text{Ln } \sigma$ and $1/T$ of $\text{Cu}_5\text{Ga}_{33}\text{Te}_{62}$ thin film at different annealing temperatures.

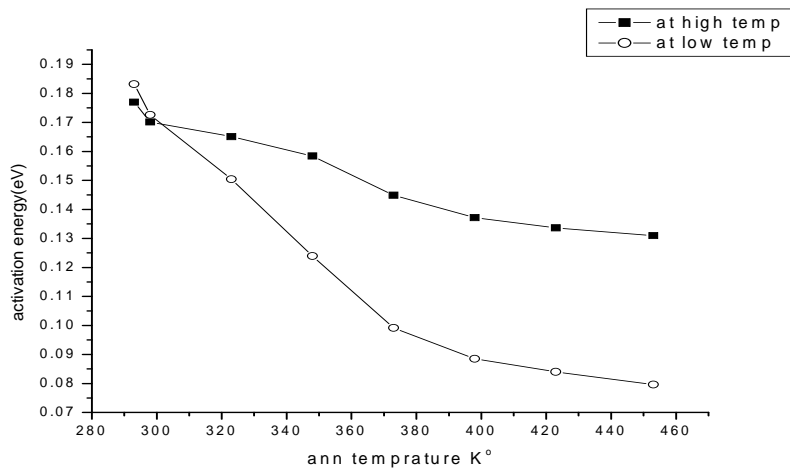


Fig. 4. The relation between the activation energy and annealing temperature in high and low regions of $\text{Cu}_5\text{Ga}_{33}\text{Te}_{62}$ thin film

3.3 Optical properties

The normal incidence transmission and absorption spectra of the thin films were measured. All optical measurements were performed at room temperature in the range 200–1100 nm by use of a double beam computer-controlled spectrophotometer. The transmission and reflection measurements were used to compute the optical energy gap and the optical constants such as refractive index n , real and imaginary parts of the dielectric constants (ϵ_r and ϵ_i) and the extinction coefficient k as expressed in the following relations[5-7].

$$\alpha = \frac{1}{d} \cdot \text{Ln} \left[\frac{(1-R)^2}{2T} + \left(\frac{(1-R)^4}{2T^2} + R^2 \right)^{1/2} \right] \quad (2)$$

$$k = \lambda \alpha / 4\pi \quad (3)$$

$$n = (R^2 - k^2) / (R^2 + k^2) \quad (4)$$

$$\varepsilon_r = n^2 - k^2 \quad \varepsilon_o = 2nk \quad (5)$$

The wavelength dependence of optical transmittance of the investigated film is shown in Fig. 5. When the annealing temperature is increased from 348 K to 453K, the film with polycrystalline structure exhibited low transmittance due to scattering and reflection of light at the grain boundaries [8]. The reflection of the annealed film increased with the annealing temperature from 348 to 453 K as indicated in Fig. 6.

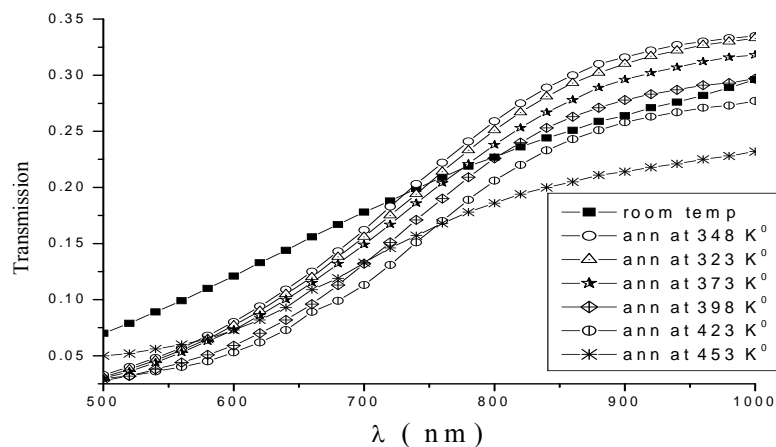


Fig. 5. The wavelength dependence of optical transmittance of $\text{Cu}_5\text{Ga}_{33}\text{Te}_{62}$ thin film at different annealing temperatures.

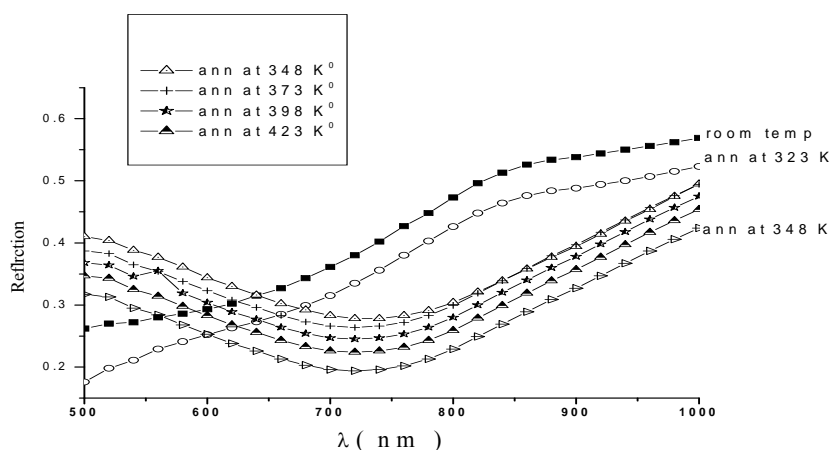


Fig. 6. the wavelength dependence of optical reflection of $\text{Cu}_5\text{Ga}_{33}\text{Te}_{62}$ thin film at different annealing temperatures

Fig.7. shows the spectrum of extinction coefficient k for the films after different T_a treatments. The k values decrease until 1.4 eV. At this energy, k was found to have nearly the same value for all annealed films. Then, it increases as the energy is raised. A similar behavior is

noticed for n , ϵ_r and ϵ_0 . Their values decrease until 1.75, 1.7 and 1.6 eV respectively. At these energies n , ϵ_r and ϵ_0 were found to have the nearly same reading for all annealed films. Then their values increase as the energy increases.

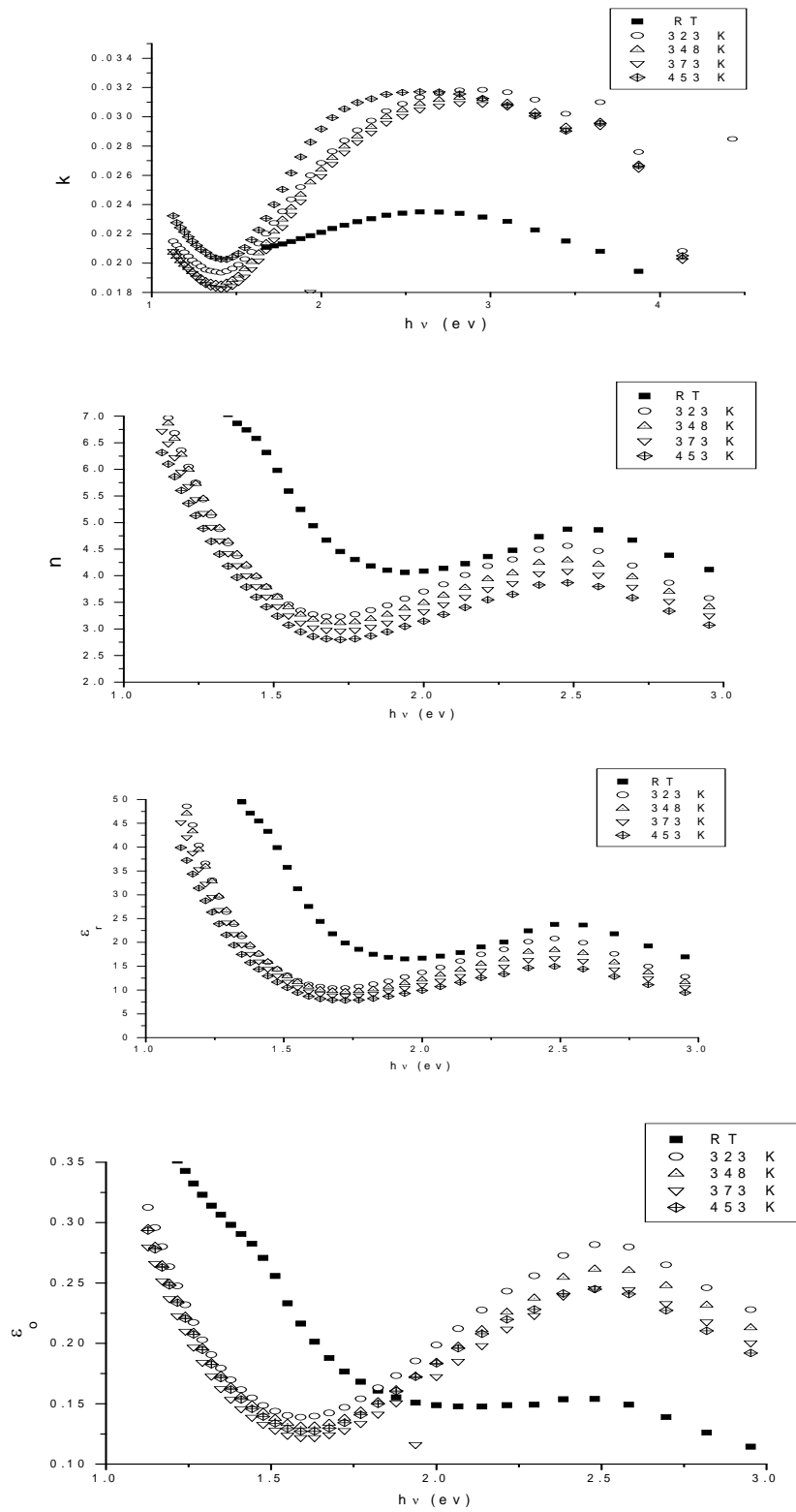


Fig.7. Variation of K , n , ϵ_r and ϵ_0 with $h\nu$ of $\text{Cu}_5\text{Ga}_{33}\text{Te}_{62}$ thin film at different annealing temperatures

The absorption coefficient (α) is related to the incident photon energy ($h\nu$) by the following equation [9]

$$\alpha h\nu = A(h\nu - E_g)^r \quad (6)$$

where A is a constant, E_g is the band gap, r is the index indicating the type of the transition. The values of r for allowed direct, allowed indirect, forbidden direct and forbidden indirect transitions are 1/2, 2, 3/2 and 3, respectively. $\text{Cu}_5\text{Ga}_{33}\text{Te}_{62}$ is direct band gap material, so putting $r = 1/2$, equation 6 can be rewritten as

$$\alpha h\nu = A(h\nu - E_g)^{1/2} \quad (7)$$

The optical band gap E_g can be obtained from the plot of $(\alpha h\nu)^2$ versus $h\nu$, as shown in Fig. 8. It can be observed that E_g decreases from 2.85 to 2.15 eV by increasing the annealing temperature from 323 to 453 K as shown in Fig.9 and Table 2.

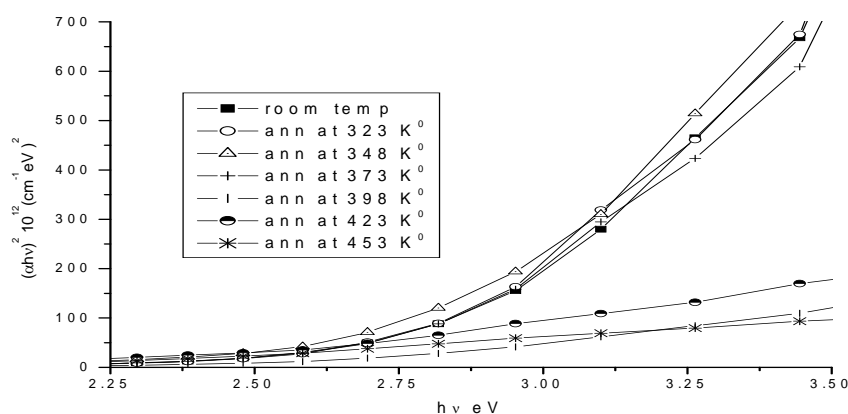


Fig.8. The optical band gap E_g obtained from the plot of $(\alpha h\nu)^2$ versus $h\nu$ of $\text{Cu}_5\text{Ga}_{33}\text{Te}_{62}$ thin film at different annealing temperatures.

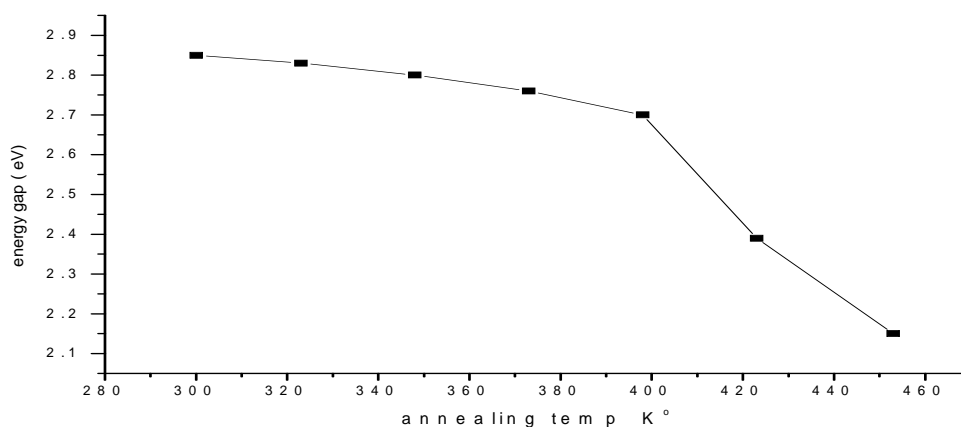


Fig.9. Variation of the optical gap with the annealing temperature of $\text{Cu}_5\text{Ga}_{33}\text{Te}_{62}$ thin film at different annealing temperatures.

Table 2. summary of the estimated values of E_g , E_o , E_d and E_e at each annealing temperature of $Cu_5Ga_{33}Te_{62}$ thin film

Annealing temperature	E_g (eV)	E_c (eV)	E_o (eV)	E_d (eV)
R.T	2.85	.022	-	-
323	2.83	.033	-	-
348	2.8	.041	2.75	15
373	2.76	.044	2.71	13.8
398	2.7	.057	2.65	11.7
423	2.39	.062	2.54	10.5
453	2.15	.083	2.4	9

As we see, the values of the energy gaps lie in the visible light, that is, For most semiconductors, gaps often lie in the range from 1 to 3 eV (in the visible regions of the spectrum) [2].

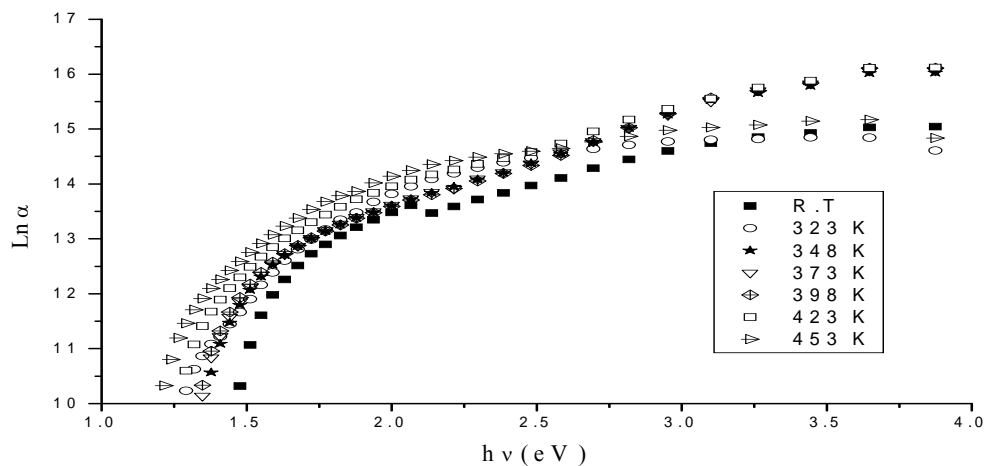


Fig.10. The relation between $Ln \alpha$ and $h\nu$ of $Cu_5Ga_{33}Te_{62}$ thin film at different annealing temperatures

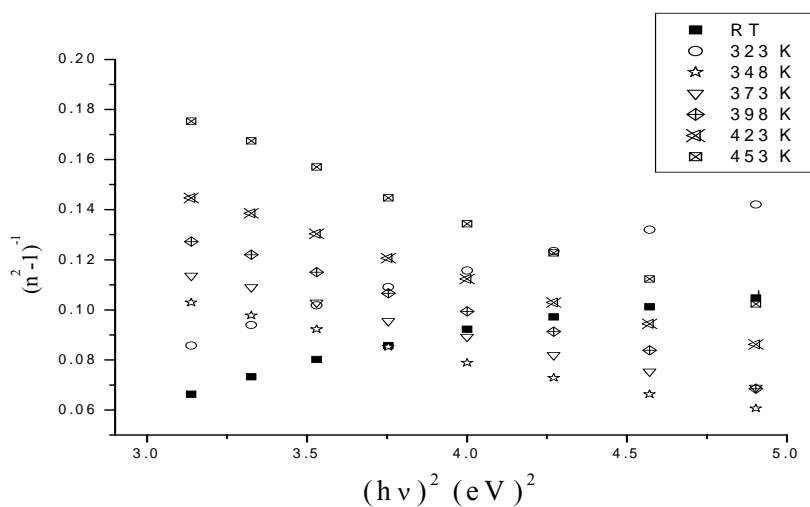


Fig.11. The relation between $(n^2-1)^{-1}$ and $(h\nu)^2$ of $Cu_5Ga_{33}Te_{62}$ thin film at different annealing temperatures

It has been noticed that, during annealing, the direct optical energy gap and electrical activation energy decrease and the width of localized states tails increases with the annealing temperature. These results can be interpreted by assuming the production of surface dangling bonds around crystallites during the process of crystallization. It has been suggested by many authors[1] that nearly ideal amorphous solids crystallize under heat treatment and that in the process of crystallization, dangling bonds are produced around the surface of the crystallites. Further heat treatment causes the crystallites to breakdown [1] into smaller crystals, thereby, increasing the number of surface dangling bonds. These dangling bonds are responsible for the formation of some types of defects in the highly polycrystalline solids. As the number of dangling bonds and defects increase with increasing the annealing temperature, the concentration of localized states in the band structure also increases gradually. Hence, the heat treatment of the films causes an increase in the energy width of localized states thereby reducing the optical energy gap and causing a rapid increase in the electrical conductivity, and consequently, a decrease in the electrical activation energy for conduction.[1]

In amorphous, as in crystalline materials, some useful information can be deduced from absorption edge measurements. Even though, in such materials the edge is less sharp than in crystals. For many amorphous materials, an exponential dependence of the absorption coefficient on photon energy $h\nu$ is found to hold over wide range and takes the form [10-12]

$$\alpha(\omega) = \alpha_0 \exp(\hbar\omega / E_e) \quad (8)$$

where α_0 is a constant, h is the reduced Planck's constant and E_e is an energy which is sometimes interpreted as the width of the tail of the localized states in the normally forbidden band gap. These are associated with the disorder of amorphous systems. The relation was first proposed by Urbach[11] to describe the absorption edge in alkali halide crystals at high absorption levels. The relation has been found to hold for many amorphous or glassy materials. Fig.10 shows the plot of $\ln \alpha$ vs photon energy. The values of E_e in equation 8 were calculated from the slopes of the straight lines of these curves near absorption edge, and are given in Table 2. From Table 2 it is clear that the width of the tail of the localized states increases with annealing temperature, which means reduction of the mobility gap. This agree well with the observed decrease of activation energy [10].

According to a single-oscillator model (Wemple -DiDomenico model [13]), the relation between the refractive index, n , and photon energy, $h\nu$, can be written as follows [8,13]

$$n = \left[1 + \frac{E_0 E_d}{E_0^2 - (h\nu)^2} \right]^{1/2} \quad (9)$$

where h is the Planck's constant, ν is the frequency, E_0 is the oscillator energy and E_d is the dispersion energy or the oscillator strength. The parameters of W-D, E_d and E_0 are related to the chemistry of the material that is E_d is related to an ionicity, anion valency, coordination number, and E_0 is related to some bond energy or bond gap, or band gap [14,15]

By plotting $(n^2 - 1)^{-1}$ against $(h\nu)^2$ and fitting a straight line as shown in Fig.11, E_0 and E_d can be determined directly from slope, $(E_0 E_d)^{-1}$, and the intercept E_0/E_d , on the vertical axis. The oscillator energy, E_0 , is an "average" energy gap and is related to the optical band gap, E_g , in close approximation by $E_0 \approx 2E_g$ [8]. In our case we find $E_0 \approx E_g$ which is in good agreement with the relation of Tichá and Tichýa [14]. Table 2 summarizes the estimated values of the oscillator parameters, E_0 , E_d and E_g .

4. Conclusions

Thin films were prepared by the thermal evaporation technique. The characteristic conductivity of $\text{Cu}_5\text{Ga}_{33}\text{Te}_{62}$ thin film annealed at different temperatures (323,348,373,398,423

and 453 K) was investigated as a function of operating temperature. The results showed that the conductivity increases with increasing annealing temperature due to transformation of the amorphous film to the crystalline state. The optical constants (refractive index n , absorption coefficient α , and extinction coefficient k) of $\text{Cu}_5\text{Ga}_{33}\text{Te}_{62}$ thin films were determined by simple straightforward calculation using transmission and reflection spectra at different annealing temperatures. The direct optical energy gap E_g and electrical activation energy E_e decrease and the width of localized states tails increases with increasing the annealing temperature. The single oscillator parameters were calculated and discussed in terms of the Wemple-DiDomenico model. The results have shown that band gap energy E_g , oscillator energy E_0 , and dispersion energy E_d are strongly dependent on the annealing temperature.

References

- [1] K. S. Bindra, Nikhil Suri, Chalcogenide Letters, **3**(9), 133 (2006).
- [2] M. Dongol, Egypt. J. Sol. **23**(2), 297 (2000)
- [3] N. F. Mott and E. A. Davis, "Electronic Process in Non-Crystalline Materials", (Clarendon Press, Oxford, 1971).
- [4] M. Farag, Journal of Material Science; Materials in Electronics, **15**, 19 (2004)
- [5] A. Alnajjar, Renewable Energy **34**, 71 (2009)
- [6] N. Mott, E. Davis, Electronic processes in non-crystalline materials, Oxford: Oxford University Press; 1979.
- [7] M. Benabdeslem et al., Solar Energy **80**, 196 (2006)
- [8] N. Tigau, V. Ciupina, Rom. Journ. Phys. **50**(7), 859 (2005)
- [9] K. D. Patel, M. S. Jani, V. M. Pathak, Chalcogenide Letters, **6**(6), 279 (2009)
- [10] A. Abdelghany, S. N. Elsayed, Vacuum, **47**(3), 243 (1996)
- [11] R. Urbach, Phys Rev. **92**, 1324 (1953)
- [12] S. K. J. Al-Ani et al., Journal of Materials Science, 661 (1985).
- [13] S. H. Wemple, Di Domenico, Phys. Rev. B, **3**, 1338 (1971).
- [14] H. Tichá, L. Tichý, J. Optoelectron. Adv. Mater. **4**(2), 381 (2002).
- [15] I. Umez, K. Miyamoto, N. Sakamoto, K. Maeda, Jpn. J. Appl. Phys. **34**, 1753 (1995).